

Multi-frame Observation-to-Orbit Association for Angles-Only Measurements

Cameron Harris, Marco Kobayashi, Jeff Houchard, Daron Nishimoto

EO Solutions Corp

Jonathan Kadan

Space Systems Command

September 2024

ABSTRACT

Within the context of space domain awareness, space traffic management, and general space object surveillance, remote sensing systems are used to collect measurements of satellite positions. Often, the identity of a satellite that produced a given measurement is not assumed *a priori*. Correct and timely identification of observed satellites is a critical endeavor of persistent monitoring and situational awareness. The fundamental procedure of determining a satellite's identity from its observed positions is referred to in this work as observation-to-orbit association. This paper presents a multi-frame observation-to-orbit data association algorithm tailored for angles-only telescope measurements. By leveraging available covariance information, the proposed method addresses the limitations that exist in other approaches in practice. Additionally, a complementary probabilistic state update method for a Kalman filter is provided, with extensibility to other state estimation techniques. The effectiveness of the association algorithm and probabilistic state update algorithms is demonstrated in two vignettes featuring multiple targets and noisy observations.

1. INTRODUCTION

Maintaining persistent knowledge of the states and identities of space objects is key to maintaining situational awareness and avoiding operational surprises in the space domain. The ever-growing population of space objects introduces greater complexity in space object monitoring and surveillance, with regards to tasking and data collection as well as data processing and exploitation. Most objects larger than a few centimeters are tracked and cataloged, and their orbital states are updated whenever new observations of the object are collected.

For general space object surveillance and identification (SOSI) systems, a network of cooperative sensors is tasked to collect observations across a catalog of space objects, judiciously scheduling tasks against object visibility windows. Multiple sensor types may constitute a SOSI network, with optical and active radar systems being typical. In the presence of tens of thousands of objects in space, observation time of individual targets is increasingly sparse, and observations may be cluttered with multiple targets. This cluttered and data-sparse environment complicates the association of observations with the corresponding cataloged target.

Multi-target tracking is an extensively published field with many applications [2]. When the source of observations is not known, some effort must be taken to determine the associated target. Within the context of space object tracking, there are three general categories of data association problems [6]: (1) observation-to-observation association, (2) observation-to-orbit association, and (3) orbit-to-orbit association.

The observation-to-observation association problem arises from the fact that sensors may collect a sequence of observations that are processed in a batch. In a cluttered tracking environment, single frames can contain multiple targets. In multi-frame processing, observation-to-observation association distinguishes which frame-by-frame detections form valid tracklets, where a "tracklet" is defined as a sequence of measurements originating from a single target over a short duration. For small timescales, a simple linear fit approach may be sufficient for observation-to-observation association, though that is not the focus of this work. Instead, this article focuses on the observation-to-orbit association problem, abbreviated as OTOA herein.

OTOA is the process of identifying a target by comparing its observed tracklet with the catalog of known objects. In the context of space object surveillance, the association of measurements to catalog objects is a critical step to enable orbit determination (OD). OD enables conjunction warnings and analysis, developing patterns of life, and other activities

DISTRIBUTION A. Approved for public release; distribution is unlimited.

Public Affairs release approval SSC/SZGA PA-899

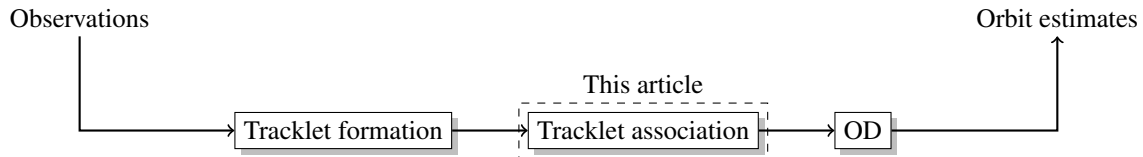


Fig. 1: Processing pipeline for incoming observations to orbit estimates. Tracklet formation involves the observation-to-observation association problem, and tracklet association involves observation-to-orbit association, the focus of this work. The pipeline concludes with orbit determination (OD) of the associated tracklets.

that require a rigorous understanding of the world state. If the track positively associates with a known target, the target’s state history may be leveraged to perform accurate OD. If the observations do not associate with any known target orbit, it is labeled as an Uncorrelated Track (UCT), and initial orbit determination (IOD) is performed to estimate its orbit.

It is assumed in this work that the initial input to OTOA is a set of tracklets, formed from a preceding tracklet formation procedure. The preceding tracklet formation step is assumed to discard false alarm detections from individual frames, so that the resulting tracklets for OTOA may be safely treated as having originated from existing space objects. The desired end state of OTOA is to determine the target associations with each tracklet. Due to kinematic and measurement uncertainties, it is possible that multiple targets associate with a given tracklet. In this case, a measure of probability must be assigned for each possible tracklet association prior to OD. The framework for the observation-to-orbit estimate pipeline assumed in this work is provided in Fig. 1.

Historically, single-frame OTOA methods have been used in SOSI systems [8]. More recently, methods of OTOA have been published that leverage IOD to transform the multi-frame observations into an orbit, whereby orbit-to-orbit association methods may be used instead [9, 12]. However, a key consideration of this method is that IOD is unreliable for noisy, short-arc angles-only measurements that are often encountered in practice.

Recognizing the criticality of OTOA in space object surveillance, it is important to have a robust OTOA method that efficiently leverages available information and minimizes failure modes. This article presents a multi-frame covariance-based OTOA method that expands on established techniques, but is compatible with all sensing modalities and suffers fewer failure modes. The focus of this article is on angles-only observations provided by optical sensors, which is the limiting case of SOSI observations. However, the proposed methodology is extensible to other measurement phenomenologies, such as radar.

2. BACKGROUND

Generally, any covariance-based association problem begins with a statistical comparison of the observed measurement \mathbf{z} with the predicted measurement of the cataloged target at observation time $\hat{\mathbf{z}}$. The difference between the predicted and observed measurement is denoted as $\tilde{\mathbf{z}}$, shown in Eq. (1).

$$\tilde{\mathbf{z}} = \mathbf{z} - \hat{\mathbf{z}} \quad (1)$$

Provided the covariance of the predicted measurement \mathbf{P}_z , it is possible to quantify the statistical variation of the observed measurement with respect to the expected distribution. Specifically, the statistical difference between the prediction and observation is the Mahalanobis distance [5], defined in Eq. (2).

$$d = \sqrt{\tilde{\mathbf{z}}^T \mathbf{P}_z^{-1} \tilde{\mathbf{z}}} \quad (2)$$

An important property of the Mahalanobis distance is that its square, d^2 , is a Chi-square distributed variable. Thus, the Chi-square statistical test for goodness of fit may be performed, as defined in Eq. (3).

$$d^2 \leq \lambda \quad (3)$$

**DISTRIBUTION A. Approved for public release; distribution is unlimited.
Public Affairs release approval SSC/SZGA PA-899**

In Eq. (3), λ is a pre-defined association gate threshold, selected from the Chi-square quantile function based on the desired significance level for the association. A typical choice for the significance level is 99%.

The null hypothesis of the chi-square test is that the sample belongs to the distribution – that is, the originator of $\hat{\mathbf{z}}$ associates with \mathbf{z} . For a catalog of targets, the OTOA procedure generally takes the form of a sequence of Chi-square tests for each target in the catalog. For a single-frame association methodology, if the test in Eq. (3) is satisfied, then the measurement is associated to the corresponding target in the catalog.

In the context of an orbit-to-orbit association problem, $\hat{\mathbf{z}}$ is the six-dimensional residual between Cartesian position and velocity, Keplerian orbital elements, or an equivalent orbital state representation. As noted before, some recent approaches to tracklet association transform the observation-to-orbit association problem to orbit-to-orbit association, facilitated by IOD of the tracklet. For angles-only measurements, traditional IOD methods include Laplace, Gauss, and Gooding algorithms [10]. Empirically, the use of IOD methods limits the data association procedure to the quality of the IOD, which may struggle to converge for short-arc angles-only measurements. Heuristic methods for OTOA have also been explored that consider look-angles instead of orbital states, but these heuristic methods do not consider state error covariances [8, 3].

3. METHODOLOGY

This article presents a multi-frame OTOA approach that operates directly on the measured values. No minimum number of measurements is required for this procedure. However, it is assumed that catalog targets have corresponding error covariance information. If a Two Line Element set (TLE) representation is available, the target's error covariance may be inferred per the analysis of Peterson *et al* [7]. It is also assumed that a Gaussian model of the covariance is valid, which may not hold for targets propagated over long timescales. The exact shelf-life of the covariance is ultimately driven by the fidelity of the force models used for propagation.

The proceeding methodology is broken out into two subsections. Section 3.1 outlines the multi-frame association procedure, tailored for angles-only measurements. Section 3.2 provides a walk-through of the probabilistic measurement update, which applies when a tracklet associates with multiple targets.

3.1 Statistical test for multi-frame association

The multi-frame association follows the same procedure outlined in Section 2, but with some modifications. For an optical angles-only measurement at time t , the two quantities measured are the object's right ascension, $\alpha(t)$, and declination, $\beta(t)$. For each target in the catalog, the target must be propagated to the measurement epoch, and the orbital state transformed to the topocentric right ascension, $\hat{\alpha}(t)$, and declination, $\hat{\beta}(t)$. Coordinate transformations from orbital state representations to topocentric right ascension and declination may be found in Vallado [10]. Following Eq. (1), the measurement residual $\mathbf{v}(t)$, also known as the innovation, is provided in Eq. (4).

$$\mathbf{v}(t) = \begin{bmatrix} \alpha(t) - \hat{\alpha}(t) \\ \beta(t) - \hat{\beta}(t) \end{bmatrix} = \begin{bmatrix} \tilde{\alpha}(t) \\ \tilde{\beta}(t) \end{bmatrix} \quad (4)$$

Instead of performing the Chi-square test on the orbital states, this method applies the Unscented Transform to the cataloged target error covariances at each measurement epoch, transforming the target error covariance in state domain to the measurement domain. Julier and Uhlmann [4] summarize the Unscented Transform to project a Cartesian error covariance to polar coordinates. In this work, the second order transformation is used, though future work may incorporate the fourth order transform, which preserves the distribution kurtosis.

The target covariance projected into the measurement domain is denoted as \mathbf{P}_y . The summation of the target error covariance \mathbf{P}_y with the sensor's own measurement error covariance \mathbf{R} yields the error covariance of the innovation, denoted here as \mathbf{S} , as shown in Eq. (5).

$$\mathbf{S}(t) = \mathbf{P}_y(t) + \mathbf{R} \quad (5)$$

Provided the innovation error covariance, the Mahalanobis distance in Eq. (2) may be calculated directly between the predicted look-angle of the cataloged target and observed look-angle.

**DISTRIBUTION A. Approved for public release; distribution is unlimited.
Public Affairs release approval SSC/SZGA PA-899**

As noted previously, the square of the Mahalanobis distance is a Chi-square distributed variable. Leveraging the additivity property of the Chi-square distribution, the Mahalanobis distances of each measurement may be summed to produce a single test statistic. This property may be leveraged to perform the association test in Eq. (3) on a tracklet rather than a single measurement. The tracklet innovation is provided in Eq. (6) for N measurements.

$$\mathbf{v}_{track} = \begin{bmatrix} \tilde{\alpha}(t_1) \\ \tilde{\beta}(t_1) \\ \tilde{\alpha}(t_2) \\ \tilde{\beta}(t_2) \\ \vdots \\ \tilde{\alpha}(t_N) \\ \tilde{\beta}(t_N) \end{bmatrix} \quad (6)$$

The error covariances for each innovation in the tracklet may be formed into a block diagonal matrix, as shown in Eq. (7).

$$\mathbf{S}_{track} = \begin{bmatrix} \mathbf{S}(t_1) & 0 & \dots & 0 \\ 0 & \mathbf{S}(t_2) & \dots & 0 \\ \vdots & \vdots & \ddots & \vdots \\ 0 & 0 & \dots & \mathbf{S}(t_N) \end{bmatrix} \quad (7)$$

Following Eq. (2), the test statistic for the track may be computed, given by Eq. (8).

$$d_{track}^2 = \mathbf{v}_{track}^T \mathbf{S}_{track}^{-1} \mathbf{v}_{track} = d_1^2 + d_2^2 + \dots + d_N^2 \quad (8)$$

The resulting test statistic d_{track}^2 has $2N$ degrees of freedom, such that $d_{track}^2 \sim \chi_{2N}^2$. The probability distribution function of d_{track}^2 is visualized for different numbers of measurements in a tracklet in Fig. 2.

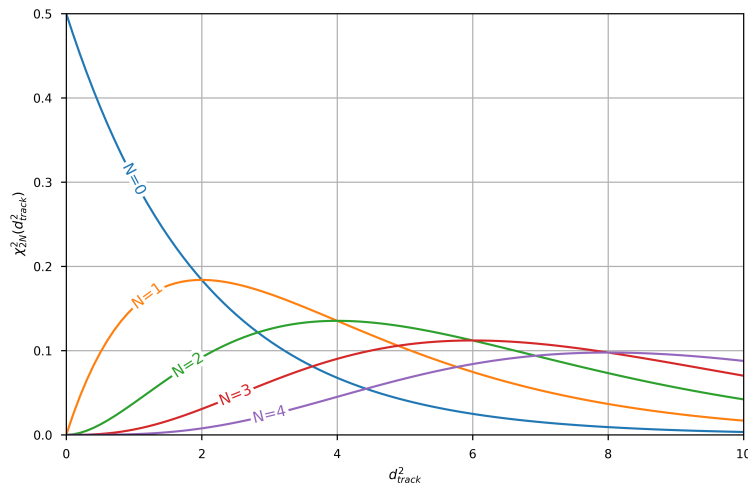


Fig. 2: Probability distribution functions for various tracklet sizes. N denotes the number of measurements constituting a tracklet.

The Chi-square test in Eq. (3) may be applied to d_{track}^2 , given an association gate λ . The value for the association gate λ should be selected based on the desired significance level from the Chi-square quantile function at $2N$ degrees of freedom. Because the number of measurements in a tracklet may vary, the value of λ will need to be selected on a per-collect basis. The outcome of the Chi-square test determines whether or not the tracklet associates with the

given catalog target. Provided a catalog of targets, the process outlined in this section is repeated for each target in the catalog. If no target in the catalog associates with the tracklet, then the tracklet is labeled as a UCT. If multiple targets associate with the tracklet, then a probabilistic measurement update may be appropriate, which is briefed in Section 3.2.

3.2 Probabilistic state update

Within the context of multi-target tracking, the states of the targets are updated as observations of the respective targets are collected. In the case that one tracklet satisfies the Chi-square test in Eq. (3) for multiple targets, a weighted state update may be performed based on the probability of the association to a given target. Note that photometric information may help identify targets in such cases if the optical signatures of the two targets are sufficiently distinct. However, association of optical signatures is not considered within the scope of this work.

Weighting the state update by the association probability ensures target state estimates do not diverge if the association is incorrect. The procedure presented here bears many similarities with the Probabilistic Data Association Filter (PDAF) described in Bar-shalom and Li [2], but leverages Bayes' theorem to further refine the association probability. The difference in the calculation of association probabilities from Bar-shalom and Li [2] results from the fact that in this work it is assumed the tracklet formation process preceding OTOA sufficiently discards false alarms in individual frames.

Take a tracklet \mathbf{Z} consisting of N angles-only measurements, such that

$$\mathbf{Z} = [\alpha_1, \beta_1, \alpha_2, \beta_2, \dots, \alpha_N, \beta_N]$$

Consider the pedagogical case where \mathbf{Z} associates with two targets. For ease of notation, the test statistic defined in Eq. (8) will be denoted as τ , such that $\tau \triangleq d_{track}^2$. The test statistics corresponding to Target 1 (T_1) and Target 2 (T_2) will be τ_1 and τ_2 , respectively. Both τ_1 and τ_2 are Chi-square distributed variables of $2N$ degrees of freedom. The probability of observing a test statistic τ_i is determined by the survival function of the Chi-square distribution at $2N$ degrees of freedom. Thus, the probability of the tracklet test statistic τ_i is given by $P(\mathbf{Z}|T_i) = \chi_{2N}^2(X > \tau_i)$.

Provided the probabilities of each distribution, a Bayesian approach can be used to calculate the likelihood that the corresponding target produced the tracklet. Each target is equally likely, as described in Eq. (9).

$$\frac{P(T_1)}{P(T_2)} = 1 \quad (9)$$

According to Bayes' theorem, the likelihood that a given target produced the tracklet is provided in Eq. (10).

$$P(T_i|\mathbf{Z}) = P(\mathbf{Z}|T_i) \frac{P(T_i)}{P(\mathbf{Z})} \quad (10)$$

The ratio of $P(T_1|\mathbf{Z})$ to $P(T_2|\mathbf{Z})$ yields Eq. (11).

$$\frac{P(T_1|\mathbf{Z})}{P(T_2|\mathbf{Z})} = \frac{P(\mathbf{Z}|T_1)P(T_1)}{P(\mathbf{Z}|T_2)P(T_2)} \quad (11)$$

Applying Eq. (9) to Eq. (11) yields Eq. (12).

$$P(T_1|\mathbf{Z}) = P(T_2|\mathbf{Z}) \frac{P(\mathbf{Z}|T_1)}{P(\mathbf{Z}|T_2)} \quad (12)$$

In this example, T_1 and T_2 are the only possible sources of the tracklet, so that $P(T_1|\mathbf{Z}) + P(T_2|\mathbf{Z}) = 1$. Algebraic manipulation and simplification of Eq. (12) produces the final association probabilities of each target, shown in Eq. (13).

$$\begin{aligned}
P(T_1|\mathbf{Z}) &= \frac{\chi_{2N}^2(\tau_1)}{\chi_{2N}^2(\tau_1) + \chi_{2N}^2(\tau_2)} \\
P(T_2|\mathbf{Z}) &= \frac{\chi_{2N}^2(\tau_2)}{\chi_{2N}^2(\tau_1) + \chi_{2N}^2(\tau_2)}
\end{aligned} \tag{13}$$

Provided the target association probability, the target's state may be updated in the catalog. Target state estimates may be maintained using some state estimation technique, typically taking the form of a least squares or Kalman filter algorithm. The Kalman filter measurement update is the focus here, considering its prevalence in space object tracking. However, the procedure may be adapted as needed to other state estimation algorithms.

The Kalman filter is a sequential estimator that applies differential corrections to an estimated state $\hat{\mathbf{x}}$. The Kalman filter algorithm ingests measurements in discrete "steps", where N measurements will correspondingly result in N filter steps, one step per measurement. For brevity, the Kalman filter algorithm will not be restated in this article, but some authoritative sources on the subject include Bar-shalom *et al* [1] and Wan and Van Der Merwe [11].

For the i^{th} target at the k^{th} filter step, the corresponding Kalman filter state update equation is provided in Eq. (14).

$$\hat{\mathbf{x}}_i(k|k) = \hat{\mathbf{x}}_i(k|k-1) + P(T_i|\mathbf{Z}) \mathbf{K}(k) \mathbf{v}(k) \tag{14}$$

In Eq. (14), $\hat{\mathbf{x}}_i(k|k-1)$ denotes the *a priori* target state estimate, $\hat{\mathbf{x}}_i(k|k)$ denotes the updated target state estimate, and \mathbf{K} denotes the Kalman gain. The scalar multiplication of $P(T_i|\mathbf{Z})$ into the state update reduces the deviation of the updated state from the *a priori* state estimate, which mitigates filter inconsistency issues if the association is incorrect. Note that $P(T_i|\mathbf{Z})$ is unchanged for the N steps involved in the filter ingestion of tracklet \mathbf{Z} for the i^{th} target, because $P(T_i|\mathbf{Z})$ quantifies the association probability for the entire tracklet \mathbf{Z} .

Provided the association probabilities, the corresponding error covariance update procedure is identical as that found in the PDAF algorithm in Bar-shalom and Li [2].

4. RESULTS

Results show considerable promise for methods presented in Section 3. The proposed algorithm has been applied to simulated collections with as many as nine different tracklets and successfully associated the observations to the correct targets. The Python implementation of the OTOA algorithm outlined in Section 3.1 can process the NORAD catalog, consisting of nearly thirty thousand objects, in less than twenty seconds on a single processor. However, it should be acknowledged that computational performance may be influenced by the available compute resources and satellite propagation theory (e.g., SGP4 vs special perturbations).

Two vignettes are provided to illustrate the utility of the multi-frame association and probabilistic state update. The first vignette in Section 4.1 demonstrates the ability of the multi-frame association to deduce target-tracklet pairings in multi-target clutter. The second vignette in Section 4.2 demonstrates the probabilistic state update for cases where there is insufficient information to form unique associations between targets and tracklets. Each vignette assumes practical, if not pessimistic, error statistics for the observed tracklets and target state covariances. The measurement error statistics are $\sigma_\alpha = \sigma_\beta = 1.5$ arcseconds in each vignette. Target state covariance sizes vary for each vignette, but follow the 10:2:1 ratio for in-track, cross-track, and radial state uncertainty, per the findings of Peterson *et al* [7].

4.1 Vignette 1 - Multi-target association

In the first vignette, two noisy tracklets of $N = 3$ measurements are present in the collect, and two targets associate with the tracklets. Target 1 is a GEO satellite, and has an uncertainty of about 10 kilometers, which may occur for targets that have been newly detected or performed a detected but unknown maneuver. Target 2 is also a GEO satellite has an uncertainty of about 2 kilometers. The scene is depicted in Fig. 3.

The legend of Fig. 3 includes the positive associations with the tracklet, based on the multi-frame association procedure outlined in Section 3.1. Following the covariance-based association, Tracklet 2 associates with both Target 1 and Target 2. However, Tracklet 1 only associates with Target 1. For $N = 3$ measurements at 99% significance, the association

**DISTRIBUTION A. Approved for public release; distribution is unlimited.
Public Affairs release approval SSC/SZGA PA-899**

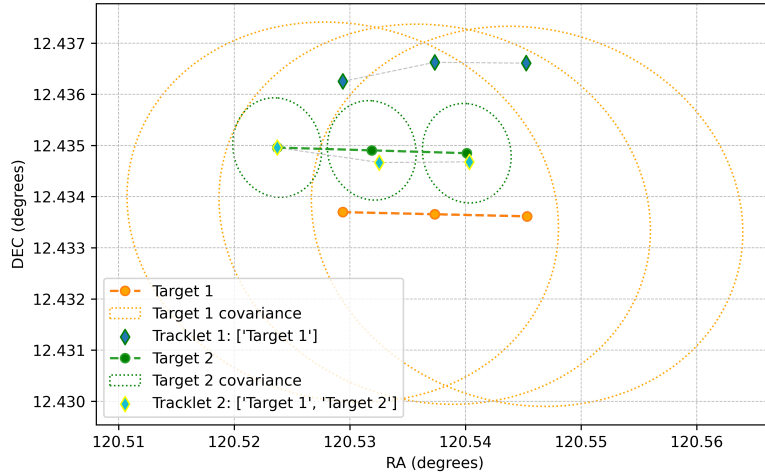


Fig. 3: Multi-target observations with varied uncertainty

gate is $\lambda = 16.8$. The test statistics for each target-tracklet pair that fell below the association gate are provided in Tab. 1.

	Tracklet 1	Tracklet 2
Target 1	3.99	1.04
Target 2	No association	0.25

Table 1: Test statistics for positive associations of target-tracklet pairs.

In terms of angular separation, Tracklet 2 is closer to Target 1 than Tracklet 1 by inspection. A heuristic association method based on tracklet distance may have associated Tracklet 2 with Target 1 and Tracklet 1 with Target 2 to minimize the combined distance between tracklets and targets, or otherwise failed to associate a target to Tracklet 1 at all. If the in-situ association algorithm fails to associate Tracklet 1 with a known target, then the typical response is to perform IOD with the collected measurements and denote the object as a UCT in the target catalog. This is an undesirable response for multiple reasons: a new unidentified object is created in the catalog, Target 1's *a priori* state is persisted in the catalog without the corrective measurement update, and analyst intervention may be required to correct the error.

Instead, consideration of error covariance reveals that Target 2 only associates with Tracklet 2, while Tracklet 1 also associates with Target 1. Thus, it follows that the originator of Tracklet 1 is Target 1, and the originator of Tracklet 2 is Target 2.

4.2 Vignette 2 - Dual association

The second vignette involves a scenario with two candidate targets at GEO altitude, but only one observed noisy tracklet. Both targets have equivalent position uncertainty of about 7 kilometers, and each have a similar association probability with the tracklet (about 50%). The scene is depicted in Fig. 4.

As before, the legend of Fig. 4 includes the positive associations with the tracklet, based on the multi-frame association procedure outlined in Section 3.1. At a significance level of 99% for $N = 5$ measurements, the association gate is $\lambda = 23.2$. Both targets associate with tracklet, and there is insufficient information to determine which target is the true originator of the tracklet. Following the probabilistic state update procedure outlined in Section 3.2, the states for both targets will be updated according to the respective association probabilities. The test statistics and association probabilities for both targets are provided in Tab. 2.

Fig. 5 compares the state errors produced by the probabilistic state update with states that either: (1) apply the “full” update (i.e., the probability weighting in Eq. (14) is ignored), or (2) receive no update. Each state is propagated two

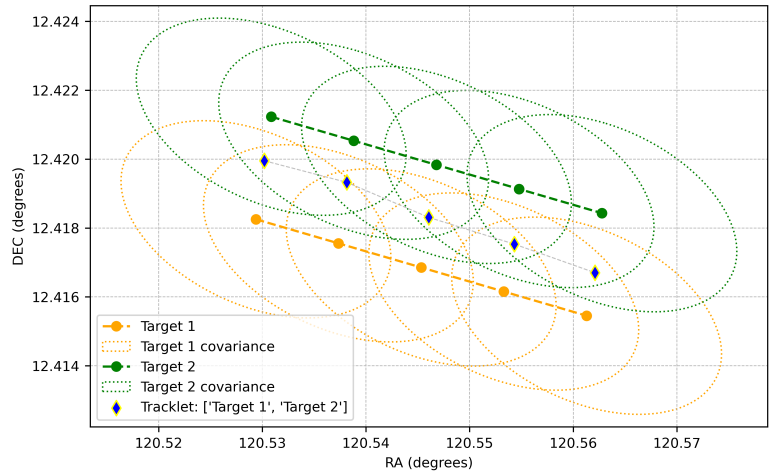


Fig. 4: A single observed tracklet with multiple associated targets

	Test statistic	Association probability
Target 1	4.14	45.4%
Target 2	3.83	54.6%

Table 2: Test statistics and association probabilities for both targets.

hours after observation to explore the ensuing effects of each choice over time. The results for Target 1 are shown in the upper plot, and for Target 2 the lower plot.

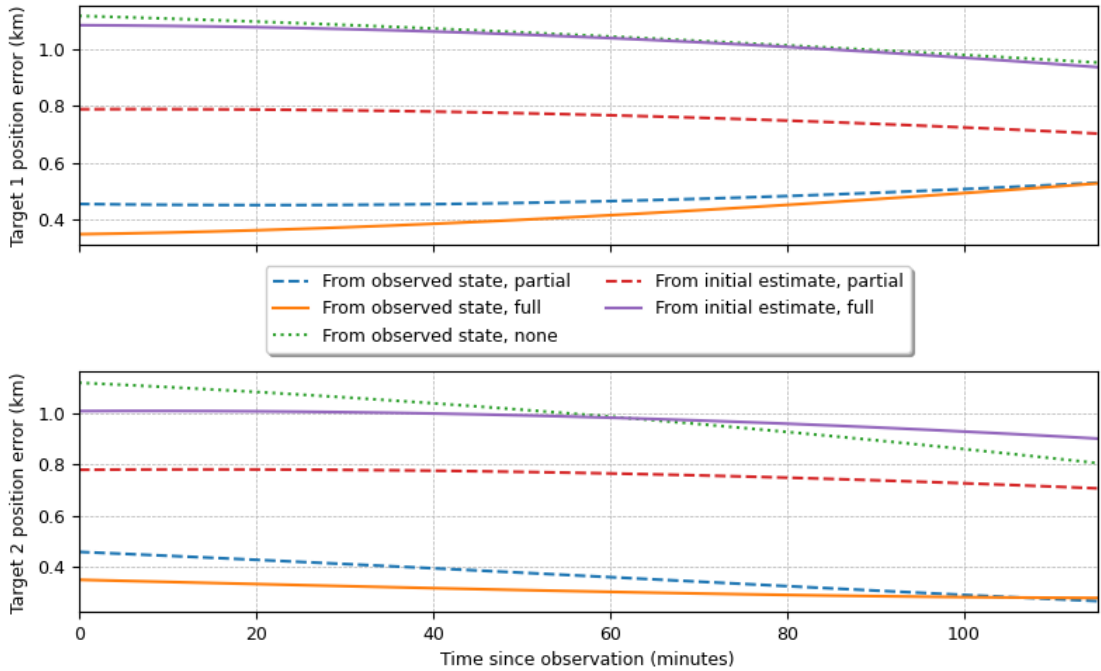


Fig. 5: Errors from propagated states resulting from different state updates

**DISTRIBUTION A. Approved for public release; distribution is unlimited.
Public Affairs release approval SSC/SZGA PA-899**

In Fig. 5, the errors “From observed state” are the Euclidean distance of the positions produced by the target estimate $\hat{\mathbf{x}}_i(k|k)$ from the true state position that produced the tracklet, which is unknown in practice. The errors “From initial estimate” are the Euclidean distance of the positions produced by the target estimate $\hat{\mathbf{x}}_i(k|k)$ from the positions produced by the prior state estimate $\hat{\mathbf{x}}_i(k|k-1)$. The “full” data points are computed with a state estimate that received the unweighted state update, the “partial” data points are computed with the weighted state update in Eq. (14), and the “none” data points are computed with no state update, such that $\hat{\mathbf{x}}_i(k|k) = \hat{\mathbf{x}}_i(k|k-1)$.

The important takeaway from Fig. 5 is that the “partial” probabilistic state update (blue) results in states with similar error from true state position to the “full” update (orange), but the “partial” states (red) deviate about 40% less than the “full” states (purple) from the *a priori* estimate. Thus, the trade-off for applying the partial update is not severe, in case the updated target is not the true originator of the observed tracklet. This is desired behavior when target associations are indeterminate.

5. CONCLUSION

Proposed in this article was a multi-frame observation-to-orbit data association procedure for noisy angles-only observations of space objects. The outlined methodology has no minimum requirements for number of observations or observation spacing, and it suffers fewer failure modes than other data association approaches in the state of practice. Preliminary results demonstrated the method is effective for determinate association of multi-target multi-tracklet scenarios and probabilistic target state updates when information is insufficient for determinate association. While the procedure was demonstrated for angles-only observations, the methodology is extensible to other measurement phenomenologies, like radar. Robust data association methods are instrumental to space surveillance as the orbital environment becomes more congested, and contemporary systems will benefit from the incorporation of trajectory uncertainties when processing cluttered observations, as demonstrated in this article.

Future work may explore feature association (such as optical signatures) for greater association confidence. Other future endeavors may explore alternative statistical goodness-of-fit tests for data association. Next steps will involve the deployment of the algorithm for on-sky testing.

6. ACKNOWLEDGEMENTS

The views expressed are those of the authors and do not reflect the official policy or position of the US Space Force, Department of Defense, or the US Government.

REFERENCES

- [1] Yaakov Bar-Shalom, X Rong Li, and Thiagalingam Kirubarajan. *Estimation with applications to tracking and navigation: theory algorithms and software*. John Wiley & Sons, 2004.
- [2] Yaakov Bar-Shalom and Xiao-Rong Li. *Multitarget-multisensor tracking: principles and techniques*, volume 19. YBS publishing Storrs, CT, 1995.
- [3] Carolin Fruh, Thomas Schildknecht, Reto Musci, and Martin Ploner. Catalogue correlation of space debris objects. In *Fifth European Conference on Space Debris*, volume 672, page 8, 2009.
- [4] Simon J Julier and Jeffrey K Uhlmann. Consistent debiased method for converting between polar and cartesian coordinate systems. In *Acquisition, Tracking, and Pointing XI*, volume 3086, pages 110–121. Spie, 1997.
- [5] Goeffrey J McLachlan. Mahalanobis distance. *Resonance*, 4(6):20–26, 1999.
- [6] Alejandro Pastor, Manuel Sanjurjo-Rivo, and Diego Escobar. Track-to-track association methodology for operational surveillance scenarios with radar observations. *CEAS Space Journal*, 15(4):535–551, 2023.
- [7] Glenn E Peterson, Robert G Gist, and Daniel L Oltrogge. Covariance generation for space objects using public data. In *Proceedings of the 11 th Annual AAS/AIAA Space Flight Mechanics Meeting, Santa Barbara, CA*, pages 201–214, 2001.
- [8] PW Schumacher Jr and DA Cooper. Angles-only data association in the naval space surveillance system. In *Proceedings of the 1994 Space Surveillance Workshop, MIT Lincoln Laboratory*, pages 5–7, 1994.

**DISTRIBUTION A. Approved for public release; distribution is unlimited.
Public Affairs release approval SSC/SZGA PA-899**

- [9] Jason Stauch, Travis Bessel, Mark Rutten, Jason Baldwin, Moriba Jah, and Keric Hill. Joint probabilistic data association and smoothing applied to multiple space object tracking. *Journal of Guidance, Control, and Dynamics*, 41(1):19–33, 2018.
- [10] David A Vallado. *Fundamentals of astrodynamics and applications*, volume 12. Springer Science & Business Media, 2001.
- [11] Eric A Wan and Rudolph Van Der Merwe. The unscented kalman filter for nonlinear estimation. In *Proceedings of the IEEE 2000 adaptive systems for signal processing, communications, and control symposium (Cat. No. 00EX373)*, pages 153–158. Ieee, 2000.
- [12] Guangyu Zhao, Lei Liu, Bin Li, Zhenwei Li, and Jizhang Sang. An orbit determination approach to associating optical tracklets of space objects. *Acta Astronautica*, 200:506–523, 2022.

**DISTRIBUTION A. Approved for public release; distribution is unlimited.
Public Affairs release approval SSC/SZGA PA-899**